Localization of Multifocal Electroretinogram Abnormalities to the Lesion Site

Findings in a Family With Best Disease

Inna V. Glybina, MD, PhD; Robert N. Frank, MD

Objective: To determine the association between multifocal electroretinogram (mfERG) abnormalities and macular lesions, as shown by retinal photography and optical coherence tomography (OCT), in a 3-generation family with vitelliform macular dystrophy.

Methods: Five family members were examined using OCT, mfERG, and retinal photography. To localize mfERG abnormalities in relation to retinal findings, we overlaid the mfERG trace arrays on the retinal images and aligned the mfERGs and OCT images in the 180° meridian.

Results: Family members had typical macular lesions, normal full-field ERGs, and reduced electro-oculogram light-dark ratios. The OCT images demonstrated variable lesion severity. Some individuals with good vision and normal-appearing fundi showed OCT abnormalities of the choroid and retinal pigment epithelium. The overlay technique revealed that the depressed mfERGs corresponded with the lesions detected by OCT and retinal photography. The latencies of mfERG components in the 2 central stimulus rings in our patients were often prolonged.

Conclusions: The mfERG abnormalities matched the localization of the macular lesions in our patients. The latencies of the mfERG N1 and P1 components in the first 2 concentric stimulus rings were often significantly (>2 SDs) delayed, an observation that has not been previously reported, to our knowledge.

Arch Ophthalmol. 2006;124:1593-1600

Author Affiliations: Kresge Eye Institute, Wayne State University School of Medicine, Detroit, Mich.

THE TERMS *BEST DISEASE* AND *vitelliform macular dystrophy* represent names for the same disorder, whose familiar nature was first described by Franz Best in 1905.[1] Like other autosomal dominant disorders, Best disease may show considerable individual variability among relatives of a single pedigree and a high degree of asymmetry between the eyes in the same affected individual.[2,3] The traditional approach in the diagnosis of Best disease has included family history, typical fundus appearance, and characteristic electrophysiological findings (abnormal electro-oculography and normal full-field electroretinography). Newer tools have recently provided additional information about the anatomical changes and physiological alterations in Best disease. These new modalities include optical coherence tomography (OCT) and multifocal electroretinography (mfERG). In this article, we show the variability of OCT and mfERG changes within a 3-generation pedigree with Best disease. Our results illustrate the range of findings of this disorder within the same family and demonstrate how these newer diagnostic modalities when used together can provide additional information about the anatomy and physiology of this disease.

METHODS

The family has been followed up by 1 of us (R.N.F.) for the last 20 years. The studies described herein were performed during their last visit in July 2005 and included OCT, mfERG, ophthalmoscopy, digital fundus photography, and visual acuity measurements. For OCT imaging, the STRATUS OCT 3 model 3000 (Zeiss-Humphrey, Dublin, Calif) was used. For mfERG recording, the VERIS system (Electro-Diagnostic Imaging, San Mateo, Calif), with a liquid crystal display monitor and a 103–hexagonal element stimulus recording protocol, was used. The luminance of the white hexagons was 200 candela (cd)/m^2, and the luminance of the black hexagons was less than 1 cd/m^2. The mean luminance of the entire screen was 100 cd/m^2. The record artifact rejection was an automatic function of the software. For the quantitative evaluation of mfERG responses, a normative database collected from healthy subjects at Kresge Eye Institute was used as a normal reference range. The database included the results of quantitative averaging of N1 and P1 amplitudes and implicit times for each mfERG concentric ring. The normative database was subdivided into separate reference groups of individuals younger than 45 years (mean ± SD age, 31.0 ± 7.8 years [age

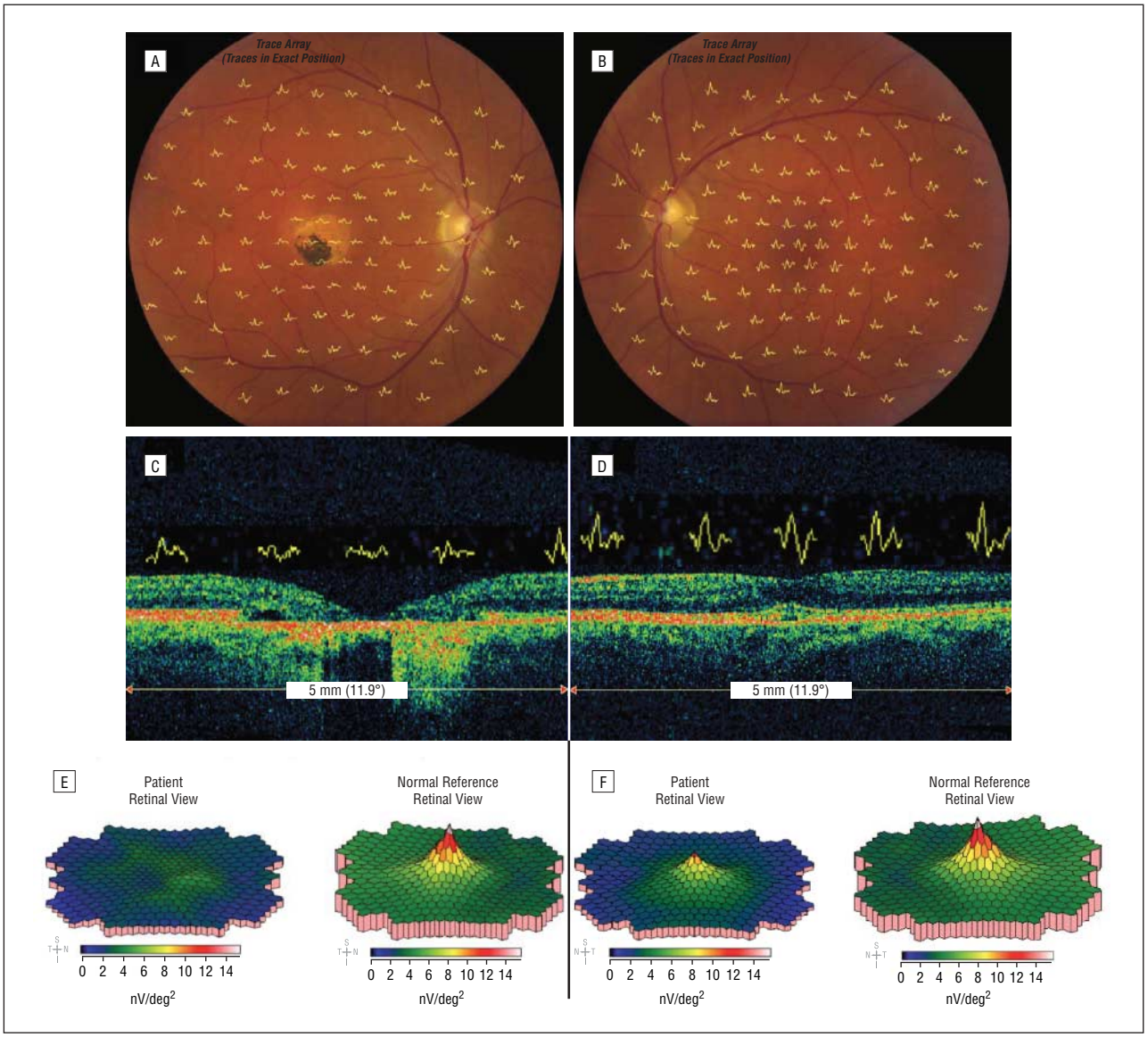

Figure 1. Patient I-1. Right eye (A) and left eye (B) fundus images with overlaid multifocal electroretinogram (mfERG) traces. Right eye (C) and left eye (D) optical coherence tomography (OCT) images at 0°, with superimposed mfERGs corresponding to the anatomical region demonstrated by OCT. Right eye (E) and left eye (F) mfERG 3-dimensional plots (left-hand panels) and 3-dimensional plots averaged from 12 age-matched healthy control subjects (right-hand panels).

range, 19-42 years]) and individuals 45 years and older (mean ± SD age, 57.0 ± 6.0 years [age range, 46-72 years]). This division into age groups was based on findings from several previous studies[4-8] of mfERG changes resulting from aging. Individuals in our normative database had refractive errors less than –5 diopters.

The mfERG response arrays were overlaid on the digital fundus photographs in the exact position of the traces. In addition, mfERG responses were aligned with the horizontal OCT images. The length of the OCT image was 5 mm, which is equivalent to 11.94° on the retina. This length covers the diameter of the first 3 mfERG concentric rings, which span 10°. The 0° (horizontal) cross-section of the OCT was used, as (because of the configuration of the 103–hexagonal element mfERG trace array) the 0° meridian is the only location where mfERG responses from all 3 central mfERG concentric rings are present in a straight line. The method of aligning the images with one another included creation of a scaling grid using Acrobat Professional 7.0 software (Adobe Systems Inc, San Jose, Calif). The scaling grid was used to allow proper correspondence of the aligned images to one another in radians.

REPORT OF CASES

Patient I-1

Patient I-1 was a 78-year-old man with a history of low vision in 1 eye since the age of 19 years. The patient had been told that he had amblyopia of uncertain etiology and was followed up with only occasional eye examinations until he was 58 years old (1985), when his 5-year-old grandson was first diagnosed with Best disease. Subsequently, all members of the family were examined.

At his visit in July 2005, the patient's best-corrected visual acuity was 20/400 OD and 20/40 OS. The patient's right eye demonstrates the atrophic stage of Best disease (**Figure 1**A). In the center of the right macula, there is a round atrophic lesion (1 disc area in size) with large irregular pigment deposits. The appearance of the

Table 1. Multifocal Electroretinogram (mfERG) N1 and P1 Amplitudes and Implicit Time Values of Patients I-1 and II-1, Compared With 18 Healthy Subjects 45 Years and Older

mfERG Index	Patient I-1		Patient II-1		Normal Values, Mean ± SD
	OD	OS	OD	OS	
First Concentric Ring					
N1 amplitude, μV	Nonmeasurable	−10.6*	−27.8	−34.2	−31.0 ± 7.8
N1 implicit time, ms	Nonmeasurable	19.2*	18.0†	20.8*	16.2 ± 1.3
P1 amplitude, μV	Nonmeasurable	25.3	17.3†	70.6	47.0 ± 17.4
P1 implicit time, ms	Nonmeasurable	31.2	30.2	33.5	31.2 ± 1.5
Second Concentric Ring					
N1 amplitude, μV	−4.8*	−11.8†	−10.8*	−23.1	−17.8 ± 3.8
N1 implicit time, ms	15.6	16.7	14.6	18.8*	16.3 ± 0.8
P1 amplitude, μV	12.4†	19.4†	15.1†	41.6	28.8 ± 9.4
P1 implicit time, ms	30.2	32.5†	31.2	32.5†	30.8 ± 0.9
Third Concentric Ring					
N1 amplitude, μV	−6.3†	−8.8†	−7.1†	−16.1	−12.7 ± 3.2
N1 implicit time, ms	15.6	15.6	14.6	16.7†	15.5 ± 0.8
P1 amplitude, μV	13.4†	14.7	18.3	30.6	21.7 ± 7.2
P1 implicit time, ms	30.2	30.2	31.2*	31.2*	30.2 ± 0.5

*Amplitude is 2 SDs below the mean, or implicit time is above the mean.
†Amplitude is 1 SD below the mean, or implicit time is 1 SD above the mean.

macula in the left eye (Figure 1B) is normal. Neither Ganzfeld ERG nor electro-oculographic (EOG) studies were performed on this patient. His diagnosis was based on family history and the presence of a macular lesion.

The mfERG showed a generalized amplitude depression of mfERG responses in the right eye. The central mfERG response (1.8° in diameter) is undetectable within the noise level (**Table 1**). The mfERG responses from the second concentric ring (5° in diameter) are depressed. In the left eye, there is a generalized slight depression of mfERG responses across the retina. The central foveal peak is depressed, and its N1 component is delayed by 3 milliseconds (>2 SDs above the mean for this age group). All 6 mfERGs from the second concentric ring are moderately depressed, and their P1 components are delayed by 2 to 3 milliseconds (approximately 2 SDs above the mean). The implicit times of mfERG responses from the third to the sixth concentric rings are within normal limits.

The OCT 5-mm horizontal image of the patient's right eye (Figure 1C) confirms the atrophic stage of Best disease, revealing marked thinning of the retina. The foveal photoreceptor layer is gone, and there is enhanced reflectivity of the choroid in that area because OCT laser beams have a shorter path through the atrophic tissue.[9] Absent or diminished mfERG responses from the same meridian correspond to the atrophic region, with absent central mfERG response occurring within the region with no photoreceptors. The depressed but still detectable mfERG response from the second concentric ring coincides with the area with a small cystoid cavity between the thinned photoreceptor layer and the retinal pigment epithelium (RPE). The 2 mildly depressed mfERGs from the third concentric ring have more normal waveforms and amplitudes. Overall, the area of advanced retinal atrophy covers the 2 central multifocal stimulus rings, including the central 5° (approximately 2 mm) in diameter.

The 5-mm horizontal image of the patient's left eye (Figure 1D) shows an early vitelliform lesion that extends from the RPE and beneath the foveolar photoreceptors. These anatomical changes correspond to the depressed amplitude of central mfERG responses, in which latencies are delayed, as are the neighboring mfERG responses from the second concentric ring.

The 3-dimensional plots on the left-hand sides of Figure 1E and F are the composite mfERG plots from the patient's right and left eyes. For comparison, the right-hand panels show mfERG 3-dimensional plots averaged from the right and left eyes of 12 healthy subjects in the same age group.

Patient II-1

The 58-year-old eldest son of patient I-1 had a history of decreased vision in his right eye since 12 years of age. At that time, he had been examined by an ophthalmologist and was told that he had a macular lesion in the right eye.

In July 2005, the patient's best-corrected visual acuity was 20/200 OD and 20/30 OS. A photograph of the posterior retina of the right eye with overlaid mfERG traces (**Figure 2**A) shows a round lesion in the fovea, approximately 1 disc area in size, with mild pigment clumping and irregular distribution of the yellow material. Ganzfeld ERG and EOG were performed in 1985. Reportedly, the ERG was normal and the EOG abnormal, but these records were unavailable.

The mfERG signals from the 3 central eccentricities are reduced. In the right eye, the foveal response is depressed, and its N1 component is delayed by 3 milliseconds. All responses from the second concentric ring are depressed. In the left eye, mfERG amplitudes of the responses from the first and second concentric rings are within the normal range. However, delays of N1 and P1

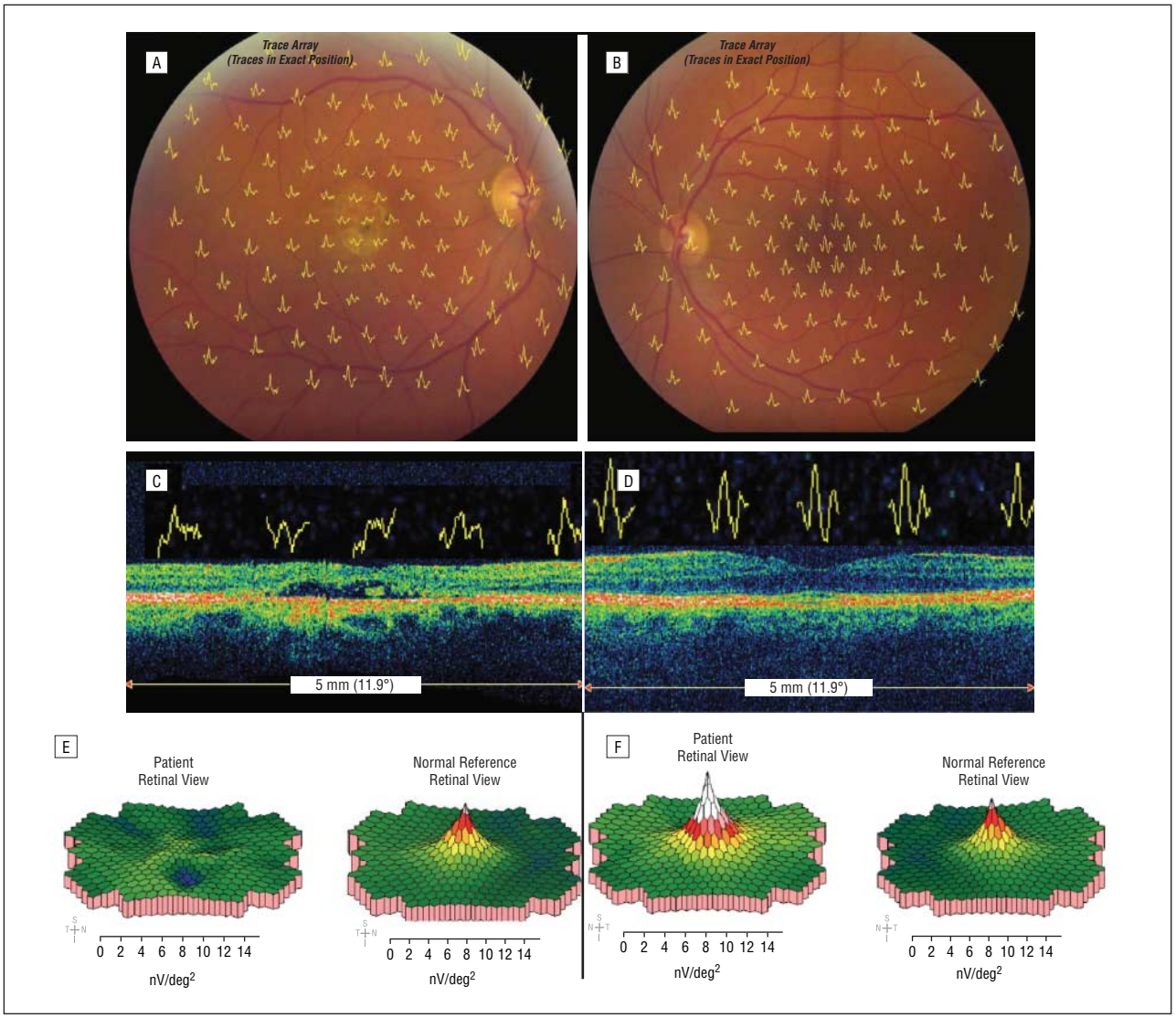

Figure 2. Patient II-1. Right eye (A) and left eye (B) fundus images with overlaid multifocal electroretinogram (mfERG) traces. Right eye (C) and left eye (D) optical coherence tomography (OCT) images at 0°, with superimposed mfERGs corresponding to the anatomical region demonstrated by OCT. Right eye (E) and left eye (F) mfERG 3-dimensional plots (left-hand panels) and 3-dimensional plots averaged from 12 age-matched healthy control subjects (right-hand panels).

are observed. The N1 component of the foveal peak is delayed by 4.6 milliseconds. The N1 components of the second concentric ring responses are delayed by 3.5 milliseconds, and their P1 components are delayed by 2 to 3 milliseconds (Table 1).

A photograph of the posterior retina of the patient's left eye appears normal (Figure 2B). The mfERG amplitudes from this eye seem to be normal throughout the tested area. However, there is a generalized delay of mfERG latencies by at least 3 to 4 milliseconds across all eccentricities, reaching 6 milliseconds in the foveal response (first eccentricity).

The horizontal 5-mm OCT image of the patient's right eye (Figure 2C) shows a subfoveal space of low reflectivity between the RPE and the photoreceptor cell layer. Within this region, the outer nuclear layer is thinned, the photoreceptors are gone, and a nodular subretinal lesion is observed in the cavity. The lesion extends over the first and part of the second central mfERG eccentricities. The mfERG responses corresponding to the lesion are affected: the first eccentricity response is undetectable; mfERGs from the second concentric ring are considerably depressed, and their P1 components are delayed by 3 to 4 milliseconds. The mfERGs from the third concentric ring, seen in Figure 2C, have normal amplitude, but their P1 components are delayed by 3 to 4 milliseconds.

The horizontal 5-mm OCT image from the left eye (Figure 2D) reveals the formation of a subfoveal schisis between the RPE and the photoreceptors, with a disruption of the photoreceptors. The first eccentricity mfERG response has normal amplitude, but its P1 component is delayed by 6 milliseconds. The responses from the second and third concentric rings, superimposed over the OCT image, also have normal amplitude, but their P1 components are delayed by 3 to 4 milliseconds.

Figure 2E and F shows the patient's right and left mfERG 3-dimensional plots (left-hand panels) compared with the 3-dimensional plots averaged from 12 age-matched healthy

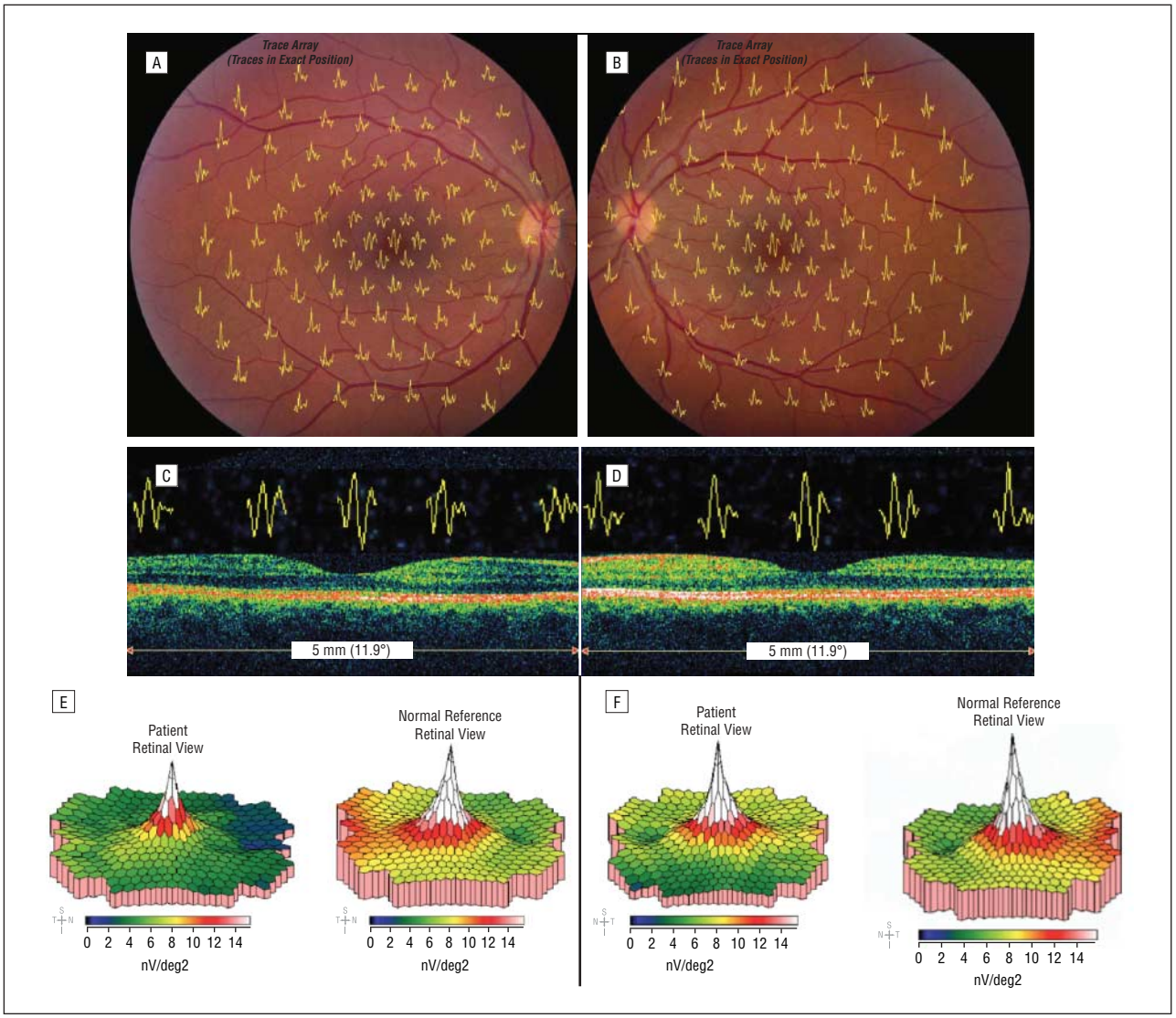

Figure 3. Patient III-1. Right eye (A) and left eye (B) fundus images with overlaid multifocal electroretinogram (mfERG) traces. Right eye (C) and left eye (D) optical coherence tomography (OCT) images at 0°, with superimposed mfERGs corresponding to the anatomical region demonstrated by OCT. Right eye (E) and left eye (F) mfERG 3-dimensional plots (left-hand panels) and 3-dimensional plots averaged from 15 age-matched healthy control subjects (right-hand panels).

control subjects (right-hand panels). The right eye response density is similar to the control plot, except for the absence of the foveal peak. In the left eye, the response density is within the normal range, and in fact the foveal peak exceeds that from the age-matched control.

Patient III-1

Patient III-1 is a 33-year-old daughter of patient II-1. Her best-corrected visual acuity was 20/25 OD and 20/25 OS. **Figure 3**A and B shows photographs of the posterior retinas of the patient's right and left eyes, with overlaid mfERG trace arrays. Both maculas appear healthy. Ganzfeld ERG and EOG recordings, performed in 1985, were normal.

The mfERG amplitudes are normal across the whole tested retina in both eyes. The slight decrease of mfERG amplitudes in the patient's right eye compared with her left eye is probably due to the patient's myopia,[10,11] which is greater in her right eye. The implicit times seem abnormal in the right and left foveal peaks. In the right foveal response, the N1 component is delayed by 3.7 milliseconds, and the P1 component is delayed by 5.2 milliseconds. In the left foveal response, the N1 component is delayed by 2.6 milliseconds, and the P1 component is delayed by 2.1 milliseconds (**Table 2**). The implicit times of the remaining mfERG traces from more peripheral eccentricities are within normal limits.

The OCT images of the right and left eyes (Figure 3C and D) show no abnormalities. The mfERG response density 3-dimensional plots of the right and left eyes, shown in Figure 3E and F, do not significantly differ from the response density values of the age-matched group of 15 healthy control subjects. This patient's EOG and full-field ERG were normal when she was first seen in 1985, and she is considered to be unaffected by Best disease.

Patient III-2

A 30-year-old daughter of patient II-1 had a normal Ganzfeld ERG and an abnormal EOG (ratios, 1.00 OD and 1.15

Table 2. Multifocal Electroretinogram (mfERG) N1 and P1 Amplitudes and Implicit Time Values of Patients III-1 and III-2 Compared With 22 Healthy Subjects Younger Than 45 Years

mfERG Index	Patient III-1		Patient III-2		Normal Values, Mean ± SD
	OD	OS	OD	OS	
First Concentric Ring					
N1 amplitude, μV	−28.9	−51.2	−11.7*	−17.7†	−31.7 ± 9.0
N1 implicit time, ms	18.8*	17.7*	16.7	20.8*	15.1 ± 1.3
P1 amplitude, μV	48.3	72.6	33.2†	35.8†	52.6 ± 15.4
P1 implicit time, ms	35.4*	32.3†	32.3†	33.3*	30.2 ± 1.4
Second Concentric Ring					
N1 amplitude, μV	−18.3	−29.0	−12.6†	−11.2†	−19.5 ± 5.7
N1 implicit time, ms	15.6	17.7†	16.7	17.7†	16.2 ± 1.1
P1 amplitude, μV	29.6	44.6	25.4	30.6	30.1 ± 9.0
P1 implicit time, ms	31.2†	30.2	32.3*	31.2†	29.8 ± 1.0
Third Concentric Ring					
N1 amplitude, μV	−14.9	−16.0	−14.2	−15.9	−13.9 ± 3.2
N1 implicit time, ms	15.6†	15.6†	15.6†	15.6†	15.0 ± 0.5
P1 amplitude, μV	21.4	35.9	22.9	32.1	21.6 ± 6.8
P1 implicit time, ms	30.2	30.2	31.2†	30.2	29.8 ± 0.8

*Amplitude is 2 SDs below the mean, or implicit time is above the mean.
†Amplitude is 1 SD below the mean, or implicit time is 1 SD above the mean.

OS) when she was first seen in 1985 at the age of 10 years. At that time, her retinas were believed to be ophthalmoscopically normal, but she had experienced symmetrically developing vitelliform macular lesions since the age of 19 years. Her best-corrected visual acuity was 20/40 OD and 20/50 OS.

A classic vitelliform stage of Best disease is present in both eyes (**Figure 4**A and B). The mfERG signals from the central 2 concentric rings are affected bilaterally. The depression of mfERG amplitude is more pronounced in the right eye, but mfERG latency delays are greater in the left eye, in which the N1 component is delayed by 5.7 milliseconds, while in the right eye it is delayed by 1.6 milliseconds. The P1 component is delayed by 2 to 3 milliseconds in both foveal responses. The P1 components of all 6 mfERG responses of the second concentric ring in each of the eyes are delayed by 2 to 3 milliseconds and are moderately reduced (Table 2). The mfERG amplitudes and implicit times across the third to the sixth concentric rings are normal in both eyes.

Horizontal 5-mm OCT images of both eyes (Figure 4C and D) show large subfoveal lesions. A low-reflective space beneath the neurosensory retina and above the RPE splits the 2 layers and elevates the neurosensory retina. The foveolar depression is absent in both eyes. The outer nuclear layer is thinned, and the photoreceptors and the RPE layer are destroyed at the lesion site in both eyes. Uniformly in both eyes, the lesion cavity is filled with a large high-reflective nodular deposit attached to the neurosensory retina. The mfERG responses seen in Figure 4C and D superimposed over the OCT image are reduced in amplitude and delayed in latency over the lesion site in both eyes. Figure 4E and F illustrates mfERG 3-dimensional response density plots for the patient's right and left eyes, compared with mfERG 3-dimensional plots averaged from the group of 22 healthy control subjects. The response densities of the foveal peaks of the patient's right and left eyes are substantially reduced, whereas the peripheral mfERG responses are slightly reduced compared with the normal reference plots, but these differences are not statistically significant.

Patient III-3

A 25-year-old son of patient II-1 was first seen in 1985 at 5 years of age. At that time, he had bilateral vitelliform macular lesions. A Ganzfeld ERG was not performed because the smallest contact lens would not fit his eyes, but the EOG ratios were abnormal at 1.32 OD and 1.52 OS. This patient was not seen for mfERG testing, which we conducted on this family in July 2005. However, at his last examination, which was earlier in 2005, his Best disease was stable at the stage of vitelliform maculopathy in both eyes, with a best-corrected visual acuity of 20/30 OD and 20/40 OS.

COMMENT

In this article, we show variations in the phenotype of Best disease within a 3-generation pedigree, a variation that is typical of many autosomal dominant disorders. Along with the anatomical and temporal variation of the disease within a single family, we demonstrate a corresponding variation in the results obtained with 2 newer diagnostic tools, OCT and mfERG. In the left eyes of patient I-1 and patient II-1, early formation of the vitelliform lesion was demonstrated by OCT, although findings from the ophthalmoscopic examination and retinal photography were unremarkable. In recent studies,[12-14] OCT was considered the method of choice in the diagnosis of Best disease. Our findings are in agreement with these reports. In the early stages of the disease in which

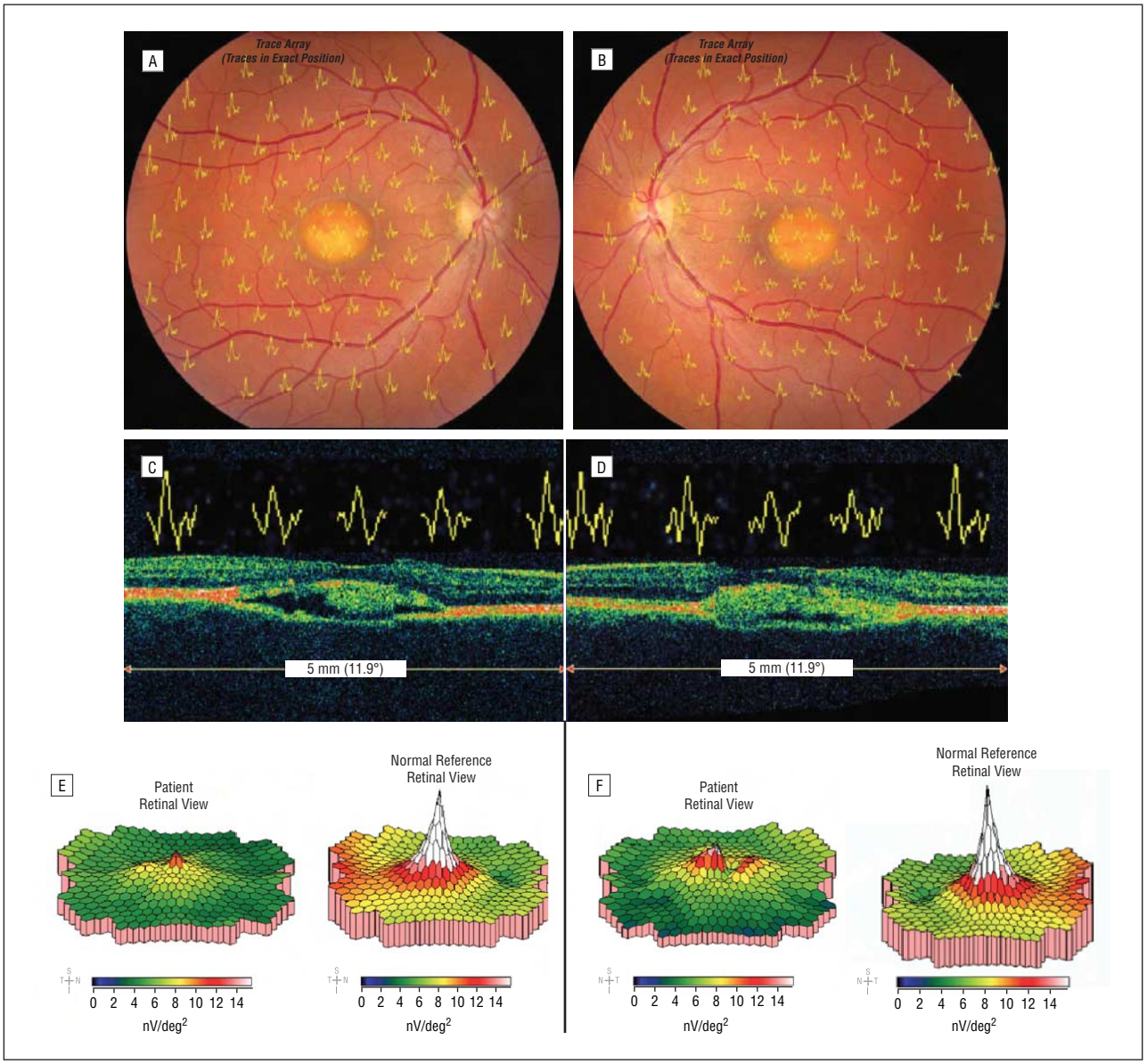

Figure 4. Patient III-2. Right eye (A) and left eye (B) fundus images with overlaid multifocal electroretinogram (mfERG) traces. Right eye (C) and left eye (D) optical coherence tomography (OCT) images at 0°, with superimposed mfERGs corresponding to the anatomical region demonstrated by OCT. Right eye (E) and left eye (F) mfERG 3-dimensional plots (left-hand panels) and 3-dimensional plots averaged from 15 age-matched healthy control subjects (right-hand panels).

the macula appears normal on opthalmoscopy, OCT reveals characteristic anatomical changes (Figure 1B and D and Figure 2B and D) such as the formation of a subfoveal cavity between the RPE and the neurosensory retina and the presence of nodular deposits in the cavity.[12-15]

In our study, mfERGs localized abnormalities in the ophthalmoscopically normal eyes that were in exact correspondence with OCT findings (Figure 1D and F and Figure 2D and F). Our composite figures show that the abnormal mfERG traces correspond precisely to the area of the lesion as shown in the retinal photographs and that the amplitude of individual mfERGs is diminished at locations with more advanced outer retinal damage, as shown in the OCT images.

Our observations of the vitelliform lesion–associated depression of mfERG amplitudes are concordant with mfERG studies[16,17] conducted using a cathode ray tube–based stimulus. In contrast to these previous studies, we found prolonged mfERG implicit times predominantly limited to the site of the ophthalmoscopically visible lesion, which lies mostly within the first 3 concentric rings. It is clear that this prolongation of the implicit times in our patients with Best disease is related to their disease and is not an artifact of our stimulation and recording system because mfERG implicit times in our control subjects, recorded with the same system, were always normal. Delays in mfERGs that we obtained from the lesion area were always observed, regardless of the depth of the lesion and without correlation to the degree of mfERG amplitude depression. Delays were 3 to 4 milliseconds for the N1 component and 3 to almost 6 milliseconds for the P1 component. Findings from recent studies[18-20] suggest that the latencies of mfERG traces are sensitive for photoreceptor and bipolar cell responsiveness because the leading slope of the P1 component is gen-

erated by ON bipolar cells, in which responsiveness might be affected primarily by damage to these cells or secondarily by an insufficient signal from damaged photoreceptors. Therefore, our patients' delayed mfERG responses might be caused by the photoreceptors and the receptive field–associated bipolar cells.

Palmowski et al[17] did not find notably prolonged mfERG implicit times among their patients with Best disease, except for 2 individuals whose N1 peak was slightly delayed within the second concentric ring. Scholl et al[16] reported significant delays ($P<.01$ to $P=.001$) in mfERG implicit times for the more peripheral third and fifth rings among patients with Best disease compared with control subjects. However, their plots show little mean difference (<1 millisecond) between the patients and controls, with considerable overlap of the standard deviations, similar to other points in their plots that are not designated as statistically significant. Variations between the results of these investigators and our findings may result from differences in values for the normative populations or from other variables that we cannot explain.

Somewhat anomalous and unexplained findings were observed in patient III-1, who has neither OCT abnormalities nor ophthalmoscopically visible retinal lesions. This patient has never had an abnormal EOG, which is considered a hallmark of Best disease. However, the latencies of her foveal mfERG responses are delayed by 3 to 4 milliseconds in both eyes. Because we have not genotyped this family, we do not know whether this patient is heterozygous for the Best disease gene but has not yet expressed (and possibly will not express) other phenotypic findings. Studies[21-23] of extensive pedigrees by several investigators show that Best disease is transmitted by a single autosomal dominant gene, with high penetrance and variable expressivity in age at onset, clinical manifestations, and rate of symptom progression, even among members of the same family. Members of a pedigree whose only clinical sign was an abnormal EOG have heretofore been designated as carriers. However, it has recently been shown in case series[23-25] by means of genotyping combined with electrophysiological examination that in some symptomatic individuals and in some asymptomatic carriers the EOG can appear normal and that the Best disease gene cannot be demonstrated in all symptomatic individuals. Although we cannot draw a definitive conclusion without genotyping, patient III-1 may represent another example of the extensive variability of expression of Best disease.

Submitted for Publication: December 23, 2005; final revision received May 11, 2006; accepted May 18, 2006.
Correspondence: Inna V. Glybina, MD, PhD, Kresge Eye Institute, Wayne State University School of Medicine, 4717 St Antoine Blvd, Detroit, MI 48201 (iglybina@med.wayne.edu).
Author Contributions: Both authors had full access to all the data in the study and take responsibility for the integrity of the data and the accuracy of the data analysis.

Financial Disclosure: None reported.
Funding/Support: This work was funded in part by a departmental unrestricted grant from Research to Prevent Blindness.

REFERENCES

1. Best F. Über eine hereditäre Makulaaffektion: Beiträge zur Vererbungslehre. *Z Augenheilkd*. 1905;13:199.
2. Gass JDM. A clinicopathologic study of a peculiar foveomacular dystrophy. *Trans Am Ophthalmol Soc*. 1974;72:139-156.
3. Lisch W. The various stages of vitelliform macular degeneration. *Klin Monatsbl Augenheilkd*. 1980;176:214-221.
4. Gerth C, Sutter EE, Werner JS. mfERG response dynamics of the aging retina. *Invest Ophthalmol Vis Sci*. 2003;44:4443-4450.
5. Fortune B, Johnson CA. Decline of photopic multifocal electroretinogram responses with age is due primarily to preretinal optical factors. *J Opt Soc Am A Opt Image Sci Vis*. 2002;19:173-184.
6. Jackson GR, Ortega J, Girkin C, Rosensteil CE, Owsley C. Aging-related changes in the multifocal electroretinogram. *J Opt Soc Am A Opt Image Sci Vis*. 2002; 19:185-189.
7. Nabeshima T. The effects of aging on the multifocal electroretinogram. *Jpn J Ophthalmol*. 2001;45:114-115.
8. Mohidin N, Yap MK, Jacobs RJ. Influence of age on the multifocal electroretinography. *Ophthalmic Physiol Opt*. 1999;19:481-488.
9. Schuman JS, Puliafito CA, Fujimoto JG. *Optical Coherence Tomography of Ocular Diseases*. 2nd ed. Thorofare, NJ: SLACK Inc; 2004.
10. Kawabata H, Adachi-Usami E. Multifocal electroretinogram in myopia. *Invest Ophthalmol Vis Sci*. 1997;38:2844-2851.
11. Kondo M, Miyake Y, Kondo N, et al. Multifocal ERG findings in complete type congenital stationary night blindness. *Invest Ophthalmol Vis Sci*. 2001;42: 1342-1348.
12. Andrade RE, Farah ME, Cardillo JA, Hofling-Lima AL, Uno F, Costa RA. Optical coherence tomography in choroidal neovascular membrane associated with Best vitelliform dystrophy. *Acta Ophthalmol Scand*. 2002;80:216-218.
13. Pianta MJ, Aleman TS, Cideciyan A, et al. In vivo micropathology of Best macular dystrophy with optical coherence tomography. *Exp Eye Res*. 2003;76:203-211.
14. Men G, Batioğlu F, Özkan SS, Atilla H, Ozdamar Y, Aslan O. Best vitelliform macular dystrophy with pseudohypopyon: an optical coherence tomography study. *Am J Ophthalmol*. 2004;137:963-965.
15. O'Gorman S, Flaherty WA, Fishman GA, Berson EL. Histopathologic findings in Best vitelliform macular dystrophy. *Arch Ophthalmol*. 1988;106:1261-1268.
16. Scholl HP, Schuster AM, Vonthein R, Zrenner E. Mapping of retinal function in Best macular dystrophy using multifocal electroretinography. *Vision Res*. 2002; 42:1053-1061.
17. Palmowski AM, Allgayer R, Heinemann-Vernaleken B, et al. Detection of retinal dysfunction in vitelliform macular dystrophy using the multifocal ERG (MF-ERG). *Doc Ophthalmol*. 2003;106:145-152.
18. Hood DC. Assessing retinal function with the multifocal technique. *Prog Retin Eye Res*. 2000;19:607-646.
19. Hood DC, Wladis EJ, Shady S, Holopigian K, Li J, Seiple W. Multifocal rod electroretinograms. *Invest Ophthalmol Vis Sci*. 1998;39:1152-1162.
20. Hood DC, Zhang X. Multifocal ERG and VEP responses and visual fields: comparing disease-related changes. *Doc Ophthalmol*. 2000;100:115-137.
21. Thorburn W, Nordstrom S. EOG in a large family with hereditary macular degeneration (Best vitelliform macular dystrophy): identification of gene carriers. *Acta Ophthalmol (Copenh)*. 1978;56:455-464.
22. Forsman K, Graff C, Nordstrom S, et al. The gene for Best macular dystrophy is located at 11q13 in a Swedish family. *Clin Genet*. 1992;42:156-159.
23. Stone EM, Nichols BE, Streb LM, et al. Genetic linkage of vitelliform macular degeneration (Best disease) to chromosome 11q13. *Nat Genet*. 1992;1:246-250.
24. Wajima R, Chater SB, Katsumi O, Mehta MD, Hirose T. Correlating visual acuity and electrooculogram recording in Best disease. *Ophthalmologica*. 1993;207: 174-181.
25. Weber BH, Walker D, Müller B, Mar L. Best vitelliform dystrophy (VMD2) maps between D11S903 and PYGM: no evidence for locus heterogeneity. *Genomics*. 1994;20:267-274.